# Electronic transitions of $C_5H^+$ and $C_5H$: neon matrix and CASPT2 studies

Jan Fulara', Adam Nagy, Arghya Chakraborty, and John P. Maier'

Citation: The Journal of Chemical Physics **144**, 244309 (2016); doi: 10.1063/1.4954703
View online: http://dx.doi.org/10.1063/1.4954703
View Table of Contents: http://aip.scitation.org/toc/jcp/144/24
Published by the American Institute of Physics

# Electronic transitions of $C_5H^+$ and $C_5H$: neon matrix and CASPT2 studies

Jan Fulara,[1,2,a)] Adam Nagy,[1] Arghya Chakraborty,[1] and John P. Maier[1,b)]
[1]*Department of Chemistry, University of Basel, Klingelbergstarasse 80, CH-4056 Basel, Switzerland*
[2]*Institute of Physics, Polish Academy of Sciences, Al. Lotników, 32/46, PL-02-668 Warsaw, Poland*

(Received 14 April 2016; accepted 13 June 2016; published online 28 June 2016)

Two electronic transitions at 512.3 and 250 nm of linear-$C_5H^+$ are detected following mass-selective deposition of $m/z = 61$ cations into a 6 K neon matrix and assigned to the $1\ ^1\Pi \leftarrow X\ ^1\Sigma^+$ and $1\ ^1\Sigma^+ \leftarrow X\ ^1\Sigma^+$ systems. Five absorption systems of $l$-$C_5H$ with origin bands at 528,7, 482.6, 429.0, 368.5, and 326.8 nm are observed after neutralization of the cations in the matrix and identified as transitions from the $X\ ^2\Pi$ to $1\ ^2\Delta$, $1\ ^2\Sigma^-$, $1\ ^2\Sigma^+$, $2\ ^2\Pi$, and $3\ ^2\Pi$ electronic states. The assignment to specific structures is based on calculated excitation energies, vibrational frequencies in the electronic states, along with simulated Franck–Condon profiles. *Published by AIP Publishing.* [http://dx.doi.org/10.1063/1.4954703]

## INTRODUCTION

Monohydrogenated polycarbons ($C_nH$) have already been detected in the interstellar medium (ISM) by radioastronomy.[1] The cosmic abundance of odd carbon systems ($C_{2n+1}H$) is found to be several times smaller than the even ($C_{2n}H$) ones.[2] The linear ($l$)-$C_5H$ molecule has been identified towards the envelope of the IRC+10 216 star *via* millimeter-wave spectroscopy.[3] Soon after, the laboratory measurements[4] consolidated the extraterrestrial identification and provided frequencies for the rotational transitions of the $^2\Pi_{3/2}$ spin-orbit component, enabling a radio detection of these in this astronomical object.[5] $l$-$C_5H$ has also been detected in TMC-1, a colder environment, where the emission lines are narrower than in the circumstellar envelope of IRC+10 216.[6] The $^{13}C$ hyperfine structure of $l$-$C_5H$ has also been investigated.[7] The $r_0$ structure could be derived from the spectroscopic constants of the isotopologues. Apart from $l$-$C_5H$, a cyclic isomer with an ethynyl group attached to a three–member carbon ring ($C_3C_2H$) has been investigated in the laboratory by microwave spectroscopy.[8]

$l$-$C_5H$, c-$C_3C_2H$, and five other isomers of $C_5H$ have been studied by *ab initio* methods[9] which show that the most stable structure is $l$-$C_5H$ and c-$C_3C_2H$ is only ~25 kJ/mol less stable. Moreover the computed geometries fit well with the molecular constants derived from the microwave spectra. The electronic transitions of the three lowest–energy isomers of $C_5H$ have been studied by the multireference configuration interaction (MRD-CI) method[10] and electronic excitation energies for $l$-$C_5H$ agree well with the experimental wavelengths recorded by a resonant two-color-two photon ionization (R2P2CI) technique.[11] However the calculations predict several electronic transitions accessible from the ground state which have not been seen in the gas-phase.[11]

In contrast to $C_5H$, little is known about the ionic counterparts: only the electronic photodetachment spectrum of $l$-$C_5H^-$[12] and computed excitation energies of $l$-$C_5H^+$ have been reported.[13] With this concern, mass-selective depositions of $C_5H^+$ in 6 K neon matrices have been undertaken and the electronic spectra of $l$-$C_5H^+$ were identified for the first time. Electronic spectra of several other $C_5H^+$ structures are also seen.

## METHODS

### Experimental

$C_5H^+$ ions were produced in a hot cathode–discharge source from the vapors of pentabromophenol (PBP) or methyldiacetylene (MDA) seeded in helium. A mixture of ions was extracted by electrostatic lenses and guided through a quadrupole bender, to eliminate neutral species, and injected to a quadrupole mass filter (QMF). After the QMF, a mass-selected beam of $C_5H^+$ was co-deposited with neon contaminated with $CH_3Cl$ in the ratio ~20 000:1 onto a rhodium coated sapphire substrate at 6 K. $CH_3Cl$ acts as an electron scavenger and suppresses neutralization of the cations. A matrix of thickness around 150 $\mu$m was grown during 3–5 hours, accumulating 30–150 $\mu$C of $C_5H^+$. A larger concentration of ions was achieved using MDA precursor as it generates $C_5H^+$ easily by dissociative ionization.

Absorption spectra were measured using a single beam spectrometer consisting of halogen or high pressure xenon lamp, a 0.3 m spectrograph, and a CCD camera. The broadband light probed the matrix through 20 mm, parallel to the substrate surface, and was then transmitted by an optical fiber to the spectrograph. The spectra were acquired in several 60–70 nm overlapping sections. The matrix was irradiated for 10–20 min with UV photons ($\lambda > 260$ nm) to neutralize the cations and the spectra were measured anew.

### Computational

Several isomers of $C_5H^+$ were chosen for the computational study (Chart 1). As a first step, the structures

a)Electronic mail: fulara@ifpan.edu.pl
b)Electronic mail: j.p.maier@unibas.ch

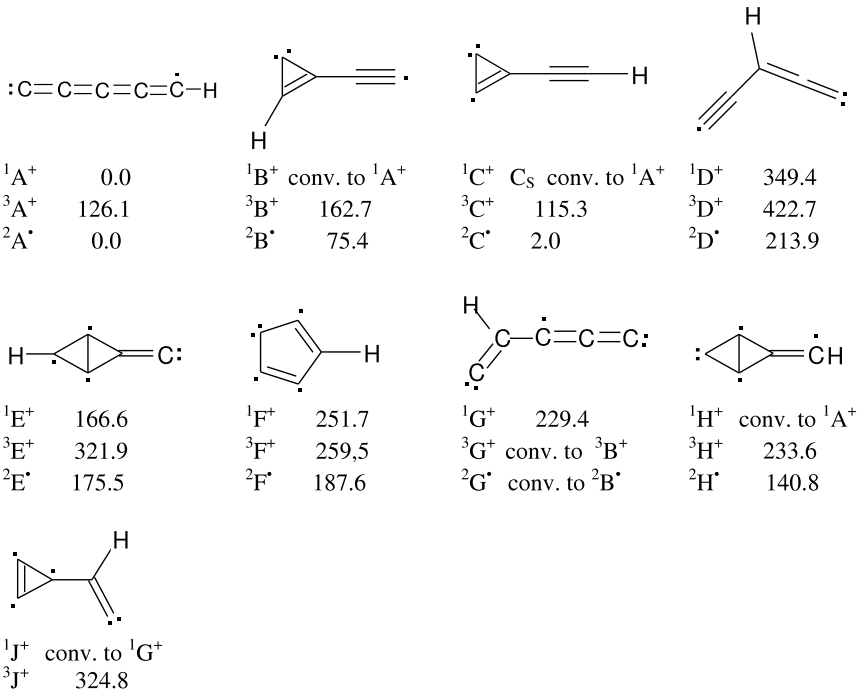


CHART 1. The relative energies (kJ/mol) of the lowest singlet and triplet isomers of $C_5H^+$ and the lowest doublets of $C_5H$ calculated at the M06-2X/cc-pVTZ level.

were examined in terms of their stability using the density functional method (DFT) with the M06-2X functional[14] and a correlation consistent basis set of triple -$\zeta$ quality (cc-pVTZ).[15] Calculations (Gaussian 09 package[16]) were carried out for the lowest singlet and triplet states of the cations and the doublet ground state of $C_5H$ neutrals. Vibrational frequencies were computed to confirm real minima. The equilibrium coordinates obtained from the DFT optimization were employed for electronic excitation energies computations. Multiconfigurational second–order-perturbation (MS-CASPT2)[17] calculations were carried out with the MOLCAS 8.0 software.[18] The active space comprises 10 electrons distributed in 11 orbitals for $C_5H^+$ and 11 electrons in 12 orbitals for $C_5H$.

## RESULTS AND DISCUSSION

### $C_5H^+$

The electronic absorption spectrum measured after deposition of mass-selected $C_5H^+$ (m/z = 61) into a 6 K neon matrix is shown as the blue trace in Figure 1 and the one obtained after exposure to UV radiation ($\lambda > 260$ nm) in red. The bands which diminish upon irradiation originate from $C_5H^+$, whereas the others gaining intensity belong to $C_5H$. Contribution from several isomers of $C_5H^+$ and $C_5H$ is evident from the spectral pattern and their different decrement upon UV exposure. Additional information is needed to attribute specific isomers of $C_5H^+$ to the particular absorption system.

A number of plausible $C_5H^+$ isomers were chosen for the geometry optimization (Chart 1). Calculations for the lowest energy singlets and triplets of nine isomers were carried out at the M06-2X/cc-pVTZ level. This reveals (Chart 1) that the linear isomer $\mathbf{A^+}$ in the singlet state is the global minimum. Four other isomers, $\mathbf{E^+}$, $\mathbf{G^+}$, $\mathbf{F^+}$, $\mathbf{D^+}$, listed in order of increasing energy have real minima on the singlet potential energy surface (PES). Structures $\mathbf{B^+}$, $\mathbf{C^+}$, and $\mathbf{D^+}$ do not have minima in the singlet state; during geometry optimization, they relax to $l$-$C_5H^+$. All nine cations except $\mathbf{G^+}$ possess real minima on the triplet PES; the latter relaxes to $^3\mathbf{B^+}$. The lowest energy structure among the triplets is $^3\mathbf{C^+}$ and $^3\mathbf{A^+}$ lies 126 kJ/mol above $^1\mathbf{A^+}$. $^3\mathbf{B^+}$ is found 163 kJ/mol above the global minimum.

Among the nine considered isomers, only $\mathbf{A^+}$, $\mathbf{E^+}$, $\mathbf{F^+}$, and $\mathbf{D^+}$ are stable in the lowest singlet and triplet states. The question arises whether the somewhat unstable cations, $\mathbf{B^+}$, $\mathbf{C^+}$, $\mathbf{G^+}$, $\mathbf{H^+}$, $\mathbf{J^+}$, can be observed in the matrix. Thus the relaxation pathway of $\mathbf{B^+}$ to $\mathbf{A^+}$ was investigated. Sections

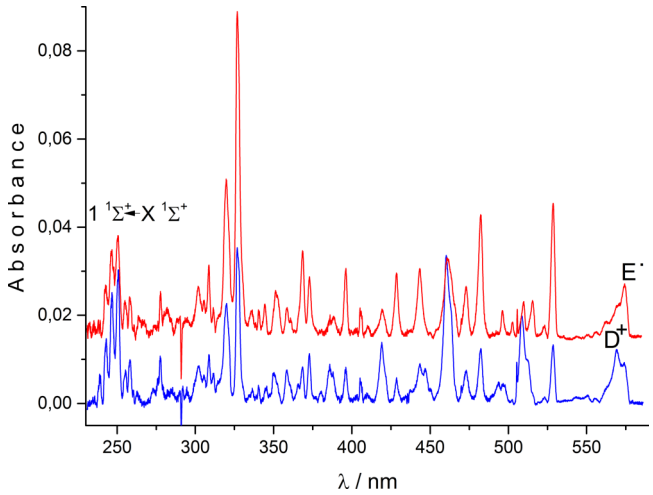


FIG. 1. Electronic absorption spectra measured after deposition of mass-selected $C_5H^+$ into a 6 K neon matrix (blue) and after irradiation with $\lambda > 260$ nm photons (red). Absorptions starting at ~250 nm are the 1 $^1\Sigma^+ \leftarrow$ X $^1\Sigma^+$ electronic transition of $l$-$C_5H^+$. Those of $\mathbf{D^+}$ and $\mathbf{E^\bullet}$ overlap around 570 nm.

of the PES of the $^3\mathbf{B}^+$ and $^1\mathbf{B}^+$ states along the deformation angle of the three-member-carbon ring leading to l-$C_5H^+$ are shown in supplementary material (Figure 1SI). The potential as a function of the distortion angle in the singlet state of $\mathbf{B}^+$ is repulsive. In the triplet state, a real minimum with a high barrier for linearization is apparent. However the energy curves of the singlet and triplet states cross near the bottom of the potential well. As a consequence, $\mathbf{B}^+$ once produced as triplet in the ion source likely relaxes fast *via* intersystem crossing to $^1\mathbf{B}^+$ and further to linear $C_5H^+$. It is unlikely that $^3\mathbf{B}^+$ will survive the fraction of a millisecond needed for the cations to travel to the matrix from the source. A similar situation prevails in case of $^3\mathbf{C}^+$. Thus only four isomers, $\mathbf{A}^+$, $\mathbf{E}^+$, $\mathbf{F}^+$, and $\mathbf{D}^+$, can be present in the matrix, of which $\mathbf{A}^+$ should be the most abundant.

Vertical excitation energies and oscillator strengths of the four $C_5H^+$ isomers computed with MS-CASPT2 are given in Table I for $\mathbf{A}^+$ and Table 1SI for $\mathbf{D}^+$, $\mathbf{E}^+$, and $\mathbf{F}^+$. The energies of several electronic transitions and their oscillator strengths for *l*-$C_5H^+$ have been calculated[13] earlier with the more sophisticated MRD-CI method and are compared with the CASPT2 predictions in Table I. A good agreement is found. A moderately intense electronic transition is expected at 2.78 eV (CASPT2) and 2.52 eV (MRD-CI) to be compared with the observation at 2.44 eV (508.7 nm). The adiabatic energy obtained with CASPT2 is 2.19 eV. A much stronger electronic transition is predicted around 5.48 eV, close to the cationic absorption (Figure 1) at 250.1 nm (4.96 eV).

The absorptions of l-$C_5H^+$ and neutrals overlap in the UV and visible. To facilitate the identification of the bands of l-$C_5H^+$ from those of neutrals, the 300–525 nm section of the spectrum measured after deposition of ions is shown in lower trace in Figure 2. The bands of l-$C_5H^+$ are marked in green and neutrals in black. The 509 nm absorption of *l*-$C_5H^+$ has an asymmetric profile with a shoulder ~140 $cm^{-1}$ to the red of the main peak. The same motif is apparent for several cationic bands marked in green in Figure 2. Therefore these absorptions belong to the same electronic system. According to the theoretical calculations the absorptions are those of the first $^1\Pi \leftarrow X\,^1\Sigma^+$ transition of *l*-$C_5H^+$ with the oscillator strength ~0.007. The main pattern in the spectrum of

TABLE I. Comparison of vertical and adiabatic excitation energies (eV) and oscillator strengths (italics) of $C_5H^+$ isomers calculated at the MS(6)-CASPT2/cc-pVTZ and MRD-CI[13] levels with the neon matrix spectra.

| | CASPT2 | | MRD-CI | | Exp. |
|---|---|---|---|---|---|
| Transitions | eV | f | eV | f | eV |
| l-$C_5H^+$ | | | | | |
| $1\,^1\Pi \leftarrow X\,^1\Sigma^+$ | 2.78 | *0.007* | 2.52 | *0.007* | 2.44 |
| | 2.19[a] | | | | |
| $1\,^1\Delta$ | 3.13 | *0* | 2.90 | *0* | |
| $1\,^1\Sigma^-$ | 3.07 | *0* | 2.98 | *0* | |
| $2\,^1\Pi$ | 5.38 | *0.003* | 5.19 | *0.001* | |
| $2\,^1\Delta$ | 5.33 | *0* | 5.20 | *0* | |
| $2\,^1\Sigma^-$ | 5.28 | *0* | 5.27 | *0* | |
| $1\,^1\Sigma^+ \leftarrow X\,^1\Sigma^+$ | 5.48 | *0.55* | 5.48 | *0.5* | 4.96 |
| $2\,^1\Sigma^+$ | 6.09 | *0.11* | 5.73 | *0.3* | |

[a]Adiabatic energy.

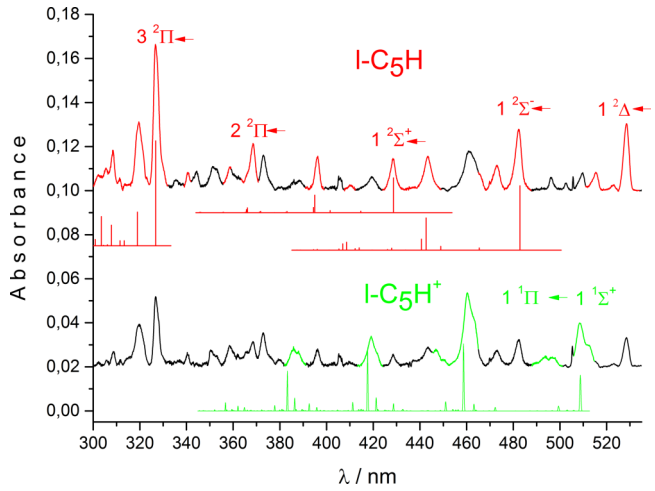


FIG. 2. Overlapping electronic absorption spectra of *l*-$C_5H$ (red) and *l*-$C_5H^+$ (green) and the assignment based on the CASPT2 excitation energies. The stick diagrams are the Franck–Condon profiles simulated with Pgopher by using totally symmetric vibrations in the ground and excited states obtained with the CASPT2 method.

*l*-$C_5H^+$ is built on two vibrational modes of energy ~600 and 2050 $cm^{-1}$, which are overtones and combination bands (Table II). The CASPT2 calculations predict three vibrations: $\nu_6$, $\nu_3$, and $\nu_2$ with frequencies 643, 1936, and 2148 $cm^{-1}$ in the $1\,^1\Pi$ electronic state close to the observation. Activity of a non-totally symmetric $\nu_6$ mode in the $1\,^1\Pi$ electronic state suggests that the strong 509 nm band may not be the origin of the system but rather the excitation of the $\nu_9$ degenerate mode. The real origin could be a shoulder (at 512.3 nm) ~140 $cm^{-1}$ to the red of the main peak. The 509 nm band and its progressions arise from Herzberg–Teller (HT) coupling of the weak $1\,^1\Pi \leftarrow X\,^1\Sigma^+$ transition with strong one ($1\,^1\Sigma^+ \leftarrow X\,^1\Sigma^+$) around 5 eV *via* the $\nu_9$ mode. The CASPT2 frequency of this mode is 111 $cm^{-1}$, not far from the observation (foot-note of Table II). Enhancement of bending motions via HT coupling is not an unusual phenomenon in carbon chains. For example, it was recently observed in the electronic spectra of $SiC_3H$ and $SiC_5H$.[19]

To resolve if the $\nu_3$ or $\nu_2$ mode is active in the spectrum a Franck-Condon (FC) simulation of the vibrational structure of the $1\,^1\Pi \leftarrow X\,^1\Sigma^+$ system was carried out using the Pgopher program[20] (green trace, Figure 2). This indicates that the $\nu_2$ mode causes the dominant progression. The $\nu_2$ antisymmetric motion leads to a compression of the C1C2 and C3C4 bonds with simultaneous expansion of the C2C3 and C4C5 bonds. Upon excitation to the $1\,^1\Pi$ state, the two former CC bonds elongate by 0.033 and 0.074 Å whereas C2C3 and C4C5 shorten by 0.046 and 0.098 Å (Table SI2). In the $1\,^1\Pi$ state *l*-$C_5H^+$ is floppy; the quasi-linear structure with a hydrogen atom ~30° off the carbon chain axis (Table 2SI) lies only 1.2 kJ/mol above the linear form. Excitation to such a non-equilibrium structure can be responsible for the broadening of the *l*-$C_5H^+$ bands.

The absorptions starting at ~250 nm (Figure 1) are assigned to the $1\,^1\Sigma^+ \leftarrow X\,^1\Sigma^+$ transition of *l*-$C_5H^+$ on the basis of the CASPT2 and MRD-CI calculations. Both methods predict a very large oscillator strength (f = 0.5). The real

TABLE II. Observed band maxima (±0.1 nm) and assignment of the $C_5H^+$ isomer absorptions and neutral counterparts in 6 K neon matrices. The assignment is based on electronic excitation energies computed and frequencies of normal modes (given in footnotes a and b and Table 5SI) in the excited electronic states for *l*-$C_5H^+$ [a] and *l*-$C_5H$[b] with the MS-CASPT2 method. The simulated Frank-Condon profiles of selected electronic transitions assisted the assignment.

| Species | λ/ nm | $\tilde{\nu}$/cm$^{-1}$ | $\Delta\tilde{\nu}$ | Assignment |
|---|---|---|---|---|
| $D^+$ | 569.1 | 17 572 | 0 | $0_0^0$ 1 $^1B_2 \leftarrow$ X $^1A_1$ |
| | 550.8 | 18 155 | 583 | $\nu_8$ |
| l-$C_5H^+$ [a] | 512.3 | 19 518 | 0 | $0_0^0$ 1 $^1\Pi \leftarrow$ X $^1\Sigma^+$ |
| | 508.7 | 19 658 | 140 | $\nu_9$ |
| | 493.6 | 20 259 | 741 | $\nu_6+\nu_9$ |
| | 460.7 | 21 706 | 2188 | $\nu_2+\nu_9$ |
| | 447.8 | 22 331 | 2813 | $\nu_2+\nu_6+\nu_9$ |
| | 419.8 | 23 821 | 4303 | $2\nu_2+\nu_9$ |
| | 386.0 | 25 907 | 6389 | $3\nu_2+\nu_9$ |
| | 250.1 | 39 984 | 0 | $0_0^0$ 1 $^1\Sigma^+ \leftarrow$ X $^1\Sigma^+$ |
| | 247.0 | 40 486 | 502 | $\nu_5$ |
| | 243.4 | 41 085 | 1101 | $2\nu_5$ |
| | 239.4 | 41 771 | 1787 | $\nu_3$ |
| $G^+$ | 372.8 | 26 824 | 0 | $0_0^0$ 4 $^1A' \leftarrow$ X $^1A'$ |
| | 365.4 | 27 367 | 543 | $\nu_7$ |
| | 358.5 | 27 894 | 1070 | $2\nu_7$ |
| $E^\bullet$ | 574.3 | 17 413 | 0 | $0_0^0$ 1 $^2A_1 \leftarrow$ X $^2B_2$ |
| | 561.6 | 17 806 | 393 | $\nu_{11}$ |
| | 556.1 | 17 982 | 569 | $\nu_6$ |
| | 301.9 | 33 124 | 0 | $0_0^0$ 4 $^2A_1 \leftarrow$ X $^2B_2$ |
| l-$C_5H$[b] | 528.7 | 18 914 | 0 | $0_0^0$ 1 $^2\Delta \leftarrow$ X $^2\Pi$ |
| | 523.1 | 19 117 | 203 | $2\nu_9$ |
| | 515.6 | 19 395 | 481 | $2\nu_8$ |
| | 473.3 | 21 128 | 2214 | $\nu_2$ |
| | 482.6 | 20 721 | 0 | $0_0^0$ 1 $^2\Sigma^- \leftarrow$ X $^2\Pi$ |
| | 465.6 | 21 478 | 757 | $\nu_5$ |
| | 443.9 | 22 528 | 1807 | $\nu_3$ |
| | 410.5 | 24 355 | 3634 | $2\nu_3$ |
| | 429.0 | 23 310 | 0 | $0_0^0$ 1 $^2\Sigma^+ \leftarrow$ X $^2\Pi$ |
| | 396.8 | 25 202 | 1892 | $\nu_3$ |
| | 368.5 | 27 137 | 0 | $0_0^0$ 2 $^2\Pi \leftarrow$ X $^2\Pi$ |
| | 344.4 | 29 036 | 1899 | $\nu_3$ |
| | 326.8 | 30 600 | 0 | $0_0^0$ 3 $^2\Pi \leftarrow$ X $^2\Pi$ |
| | 320.0 | 31 250 | 650 | $\nu_5$ |
| | 309.0 | 32 363 | 1763 | $\nu_3$ |
| | 305.7 | 32 712 | 2112 | $\nu_2$ |

[a]l-$C_5H^+$ X $^1\Sigma^+$; $\nu_1-\nu_9$: 3404, 2185, 2063, 1449, 773, 722, 551, 273, 123. 1 $^1\Pi$; $\nu_1-\nu_9$: 3367, 2148, 1936, 1524, 766, 643, 462, 371, 111.
[b]l-$C_5H$ X $^2\Pi$; $\nu_1-\nu_9$: 3500, 2023, 1936, 1434, 756, 626, 584, 298, 138. 1 $^2\Delta$; $\nu_1-\nu_5$: 3497, 2048 , 1759, 1470, 747. 1 $^2\Sigma^-$; 3507, 1986, 1887, 1567, 778. 1 $^2\Sigma^+$; 3508, 2018, 1984, 1569, 783. 3 $^2\Pi$; 3495, 2345, 1883, 1314, 750.

intensities of the bands in this spectral range are likely larger than observed due to enhanced light scattering in the UV. In this region, a portion of light after passing through the entrance slit and a fraction of its path in solid neon escapes the matrix and is reflected from the metal surface within the chamber. It can re-enter the matrix near the exit slit of the system. In effect the effective light path is shorter than at longer wavelengths and absorptions are weaker. Two weak bands at 257.9 and 254.2 nm seen in Figure 1 likely belong to another transition of l-$C_5H^+$. The calculations predict a much weaker 2 $^1\Pi \leftarrow$ X $^1\Sigma^+$ transition at 5.38 eV (Table I).

Besides the absorptions assigned to *l*-$C_5H^+$, a weak cationic band around 570 nm, which overlaps with a neutral feature, is seen (blue trace, Figure 1). According to the CASPT2 calculations (Table 1SI) among the three higher-energy isomers of $C_5H^+$, **D$^+$**, **E$^+$**, and **F$^+$**, only the former has a moderately intense electronic transition at 2.22 eV (559 nm) close to this wavelength. Therefore the absorptions starting at 569.1 nm are assigned to the 1 $^1B_2 \leftarrow$ X $^1A_1$ system of **D$^+$**. Two weaker electronic transitions are expected at 2.54 (488 nm) and 3.06 eV (405 nm) (Table 1SI); however, absorption features weaker than that at 569 nm cannot be distinguished in the blue trace of Figure 2 due to congestion in this region.

## $C_5H$

One can anticipate that *l*-$C_5H$ is the main isomer formed upon neutralization because the absorptions of *l*-$C_5H^+$ dominate the spectrum measured after accumulation of $m/z = 61$ ions (blue trace, Figure 1). Hence the bands which gain in intensity after irradiation of the matrix with $\lambda > 260$ nm photons are likely to be absorptions of *l*-$C_5H$ (red trace). The electronic spectrum of *l*-$C_5H$ has been measured in the gas phase by a mass-selective R2P2CI technique and two electronic transitions at 532.2 and 485.2 nm reported.[11] The wavelengths are close to the absorption bands at 528.7 and 482.6 nm in the neon matrix. The gas phase-matrix shifts (3.5 and 2.6 nm) lie within 1% of the excitation energy as has been documented for a range of molecules.[21] The absorptions starting at 528.7 and 482.6 nm are assigned to two electronic systems of l-$C_5H$.

Vertical excitation energies and oscillator strengths have been computed with MS(6)-CASPT2 using coordinates from the M06-2X/cc-pVTZ calculations to map the other electronic transitions of *l*-$C_5H$. The $C_{2v}$ symmetry had to be used for technical reasons. The SCF orbitals are shown in Figure 2SI. The ground state configuration is $(\ldots)(1b_1)^2(1b_2)^2(11a_1)^2(2b_1)^2(2b_2)^2(3b_1)^1$ or in a more compact form, 20 22u00 22 000, and the resulting ground electronic state is X $^2\Pi$. Promotion of one electron from the $11a_1$ orbital to $3b_1$ and/or $3b_2$ leads to two electronic states of $a_1$ symmetry with the main configurations: u0 22 200 22 000 and u0 22 000 222 000 and reference weight (r.w.) = 0.38, and two states of $a_2$ symmetry with the main configurations: u0 22d00 22u00 and u0 22u00 22d000. The first electronic states of $a_1$ and $a_2$ symmetry have the same energy 2.35 eV and correspond to the 1 $^2\Delta$ state in $C_{\infty v}$. The second states of $a_2$ and $a_1$ symmetry at 2.56 and 2.90 eV transform to 1 $^2\Sigma^-$ and 1 $^2\Sigma^+$.

The CASPT2 results are compared with the earlier MRD-CI calculations[10] in Table III and a good agreement is apparent. Both theoretical methods predict a number electronic states accessible from the X $^2\Pi$ state by optical excitation, e.g., in the visible three transitions to the 1 $^2\Delta$, 1 $^2\Sigma^-$ and 1 $^2\Sigma^+$ electronic states are expected. The proximity of the excited electronic states causes an overlap of the absorption bands. The FC simulations have been carried out to assign the observed bands to a specific electronic transition. The vibrational profiles are compared with the neon matrix spectrum in Figure 2. From the calculated excitation energies, the absorption features starting

TABLE III. Comparison of vertical excitation energies (eV) and oscillator strengths (italics) of $C_5H$ isomers calculated at the MS(6)-CASPT2/cc-pVTZ and MRD-CI[10] levels with the neon matrix spectrum.

| Transitions | CASPT2 | | MRD-CI | | Exp. |
|---|---|---|---|---|---|
| l-$C_5H$ | | | | | |
| 1 $^2\Delta \leftarrow X\,^2\Pi$ | 2.35 | *0.003* | 2.54 | *0.003* | 2.35 |
| 1 $^2\Sigma^-$ | 2.56 | *0.007* | 2.71 | *0.009* | 2.57 |
| 1 $^2\Sigma^+$ | 2.90 | *0.003* | 3.09 | *0.005* | 2.89 |
| 1 $^2\Pi$ | 2.95 | *0.0004* | 3.11 | *0.001* | |
| 2 $^2\Pi$ | 3.75 | *0.015* | 4.00 | *0.007* | 3.36 |
| 3 $^2\Pi$ | 4.11 | *0.032* | 4.13 | *0.03* | 3.79 |
| 2 $^2\Sigma^-$ | 4.73 | *0.003* | 5.00 | *0.001* | |

at 528.7 nm (2.34 eV) and 482.6 nm (2.57 eV) are assigned to 1 $^2\Delta \leftarrow X\,^2\Pi$ and 1 $^2\Sigma^- \leftarrow X\,^2\Pi$ transitions, respectively (Table II). This is in agreement with the interpretation made previously on the basis of CASSCF calculations.[11] A slightly weaker absorption is observed at 429.0 nm (2.89 eV) close to the energy 2.90 eV predicted for the 1 $^2\Sigma^+$ state and thus attributed to the 1 $^2\Sigma^+ \leftarrow X\,^2\Pi$ system.

Promotion of an electron from the $3b_1$ ($\pi_x$) to higher $\pi$ orbitals leads to a number of $^2\Pi$ electronic states (Figure 2SI). The strongest electronic transition (f = 0.03) from X $^2\Pi$ is predicted to the 3 $^2\Pi$ state at around 4 eV. The energy matches well the origin of the strongest absorptions of neutral $C_5H$ at 327 nm (3.79 eV) (Figure 2). Moreover, the FC profile of the 3 $^2\Pi \leftarrow X\,^2\Pi$ system mimics the experimental spectrum. A weaker 2 $^2\Pi \leftarrow X\,^2\Pi$ transition at 3.75 eV is also detected (Figure 2) with onset at 368 nm (3.36 eV). In the gas-phase R2P2CI experiments,[11] the wavelength region down to 330 nm was covered; however, no additional absorptions of l-$C_5H$ were detected. This suggests a short lifetime in the 1 $^2\Sigma^+$, 2 $^2\Pi$, and 3 $^2\Pi$ electronic states resulting from fast internal conversion.

In the spectrum recorded after neutralization of $C_5H^+$ (red trace, Figure 1), apart from the absorptions in the 320-530 nm range assigned to the electronic transitions of *l*-$C_5H$, weak features with onset at 574 nm (2.16 eV) are apparent. No electronic states of *l*-$C_5H$ are expected below 1 $^2\Delta$ and hence the absorptions are due to another isomer of $C_5H$. To identify these, vertical excitation energies of several $C_5H$ isomers have been computed with the MS(6)-CASPT2 (11/12) method. Though production of the cationic precursors of $^2$**B**$^\bullet$ and $^2$**C**$^\bullet$ are not favored under the experimental conditions (*vide infra*), the calculations were also performed for these neutrals and the results are compared in Table 3SI with those obtained with MRD-CI.[10] For the remaining species, $^2$**D**$^\bullet$, $^2$**E**$^\bullet$, and $^2$**F**$^\bullet$, the results are collected in Table 4SI. The agreement between the CASPT2 and MRD-CI results is reasonable; hence one can expect that the excitation energies of **D**$^\bullet$, **E**$^\bullet$, and **F**$^\bullet$ are predicted with the same accuracy as for **B**$^\bullet$ and **C**$^\bullet$. Only the three isomers, **B**$^\bullet$, **E**$^\bullet$ and **F**$^\bullet$, possess electronic transitions near the 574 nm (2.16 eV) system. In the case of **B**$^\bullet$, the CASPT2 energy of 1.80 eV is 0.4 eV below the observation and MRD-CI by 0.5 eV. One can exclude **B**$^\bullet$ as the carrier due to the large difference between the experimental and calculated energies and unfavorable production of **B**$^+$. The three electronic transitions with energies 1.65, 2.00, and 2.22 eV having similar intensities are predicted for **F**$^\bullet$, whereas only one absorption system is detected in this range. Hence this isomer can also be ruled out. A moderately intense (f = 0.005) electronic transition is expected around 2.15 eV for **E**$^\bullet$. Its strongest transition (f = 0.024) lies around 5.70 eV (218 nm), beyond the detection range of the apparatus. Another, moderately intense transition of **E**$^\bullet$ is predicted by CASPT2 (Table 4SI) at ~4.34 eV close to the position of the neutral absorption at 301.9 nm (4.11 eV). In view of the proximity of the calculated and experimental energies, and the fact that there are no other competing isomers, the 574 nm system and the 301.9 nm band are assigned to the 1 $^2A_1 \leftarrow X\,^2B_2$ and 4 $^2A_1 \leftarrow X\,^2B_2$ electronic transitions of **E**$^\bullet$, respectively.

## Photo-induced band system at 373 nm

Irradiation of the matrix containing $C_5H^+$ with 300 < λ < 400 nm photons resulted in the appearance of new absorptions starting at 373 nm (green trace, Figure 3). The spectra measured after deposition of $C_5H^+$ (blue trace) and the one obtained after neutralization of the cations (red trace) are shown for a comparison. The first irradiation (300 < λ < 400 nm) induces only a slight change in the intensity of the cationic absorptions and those of neutral *l*-$C_5H$. The former diminish and the latter increase due to a partial neutralization of the cations at these wavelengths. The threshold for the appearance of the 373 nm absorption system lies around 340 nm. Neutralization of the cations cannot take place energetically with 340 nm photons and no difference is observed in between the spectra measured after deposition and after the first irradiation except in the region where the new absorptions appeared. The 373 nm system ultimately decreased after the second irradiation (λ > 260 nm) implying its cationic origin.

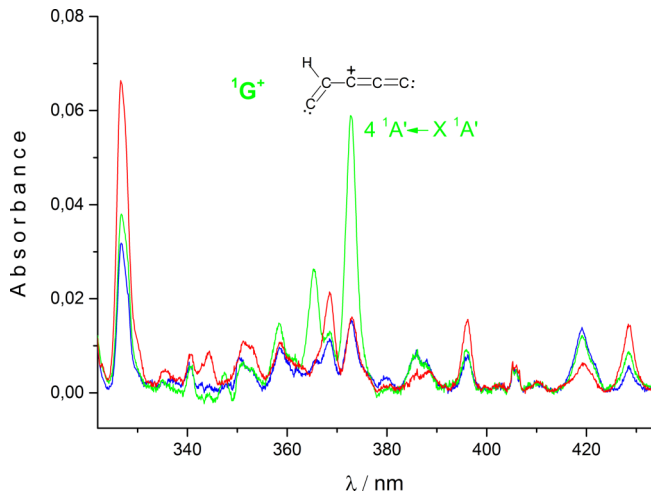


FIG. 3. The section of the absorption spectrum of $C_5H^+$ measured after deposition of the cations into solid neon (blue) and after subsequent exposure to 290 < λ < 390 nm photons (green). The red trace is the spectrum of $C_5H$ recorded after neutralization of the cations with λ > 260 nm photons. The band of *l*-$C_5H^+$ around 420 nm slightly decreases in intensity and the ones of neutral l-$C_5H$ e.g., at 303 nm slightly increase after the first irradiation. The green trace is the 4 $^1$A′ ← X 1A′ electronic transition of $^1$**G**$^+$.

A dissociation product of $C_5H^+$ can be excluded from the consideration for the following reasons. The new absorptions starting at 372.8 nm are unique for deposition of $C_5H^+$ ions. The 373 nm system is not observed in mass-selected experiments with $C_5H_2^+$, $C_5H_3^+$, $C_5^+$, $C_4^+$, $C_4H^+$, and smaller ions. A larger, dimer-like molecule can also be excluded due to a very large dilution of ions in a neon matrix (~1:$10^6$). Therefore the 373 nm system originates from a photo-unstable $C_5H^+$ cation produced in the matrix upon ~340 nm light exposure. The precursor should possess a transition in the 300-400 nm range with a low oscillator strength and/or broad absorption, because no band which decays with the appearance of 373 nm (3.33 eV) system was seen. $^3$**B**$^+$ and $^3$**C**$^+$ are ruled out for the reason discussed in preceding paragraphs and because their strongest electronic transitions lie elsewhere (Table 1SI). A reasonable candidate is isomer $^1$**G**$^+$ which possesses a relatively intense 4 $^1$A′ ← X $^1$A′ (f = 0.04) transition at 3.81 eV. **G**$^+$ cannot be formed in the ion source due to preferential formation of *l*-$C_5H^+$, but in the confined matrix environment, it is generated *via* photo-isomerization and can be stabilized.

## CONCLUSIONS

*l*-$C_5H^+$ is the most abundant ion of $m/z$ = 61 produced in a discharge source from methyldiactylene or pentabromophenol vapors. *l*-$C_5H^+$ is the global minimum on the PES. Two moderately intense electronic transitions of *l*-$C_5H^+$ near 512 and 250 nm are detected; absorptions of two higher–energy isomers **D**$^+$ and **G**$^+$ are also observed. **G**$^+$ is energetically unstable under normal conditions and appears to be photo-generated in the matrix upon UV-exposure. Neutralization of the cations led to numerous absorptions of *l*-$C_5H$ in the 300–530 nm region and weak features of **E**$^•$ commencing at 574 nm.

The results reported in this paper can be used as a guide for gas–phase studies of *l*-$C_5H^+$ and for the higher–energy electronic transitions of *l*-$C_5H$. These may be of astrophysical interest. The microwave detection of *l*-$C_5H^+$ in the ISM is restrained due to the ~30% smaller dipole moment than of *l*-$C_5H$. As an alternative, an extraterrestrial detection of *l*-$C_5H$ could use the **3** $^2\Pi \leftarrow X\ ^2\Pi$ transition at 327 nm and for *l*-$C_5H^+$ the **1** $^1\Sigma^+ \leftarrow X\ ^1\Sigma^+$ absorption at 250 nm.

## SUPPLEMENTARY MATERIAL

See supplementary material for the potential energy curve of the lowest singlet and triplet of isomer $B^+$ (Figure S1), the HOMO and LUMO orbitals, and discussion of the electronic configurations of the excited states of l-$C_5H$ (Figure 2SI), excitation energies and oscillator strengths of $C_5H^+$ isomers (Table 1SI), optimized coordinates of l-$C_5H^+$ in the X $^1\Sigma^+$ and 1 $^1\Pi$ electronic states (Table 2SI), excitation energies and oscillator strengths of neutral isomers of C5H (Tables 3SI and 4SI), and vibrational frequencies of $C_5H^+$ and C5H (Table 5SI).

## ACKNOWLEDGMENTS

This work was supported by the Swiss National Science Foundation (Project No. 200020-124349/1). Calculations were performed at sciCORE (http://scicore.unibas.ch/) scientific computing core facility at University of Basel.

[1]M. B. Bell, P. A. Feldman, J. K. G. Watson, M. C. McCarthy, M. J. Travers, C. A. Gottlieb, and P. Thaddeus, Astrophys. J. **518**, 740 (1999).
[2]M. Guélin, J. Cernicharo, M. J. Travers, M. C. McCarthy, C. A. Gottlieb, P. Thaddeus, M. Ohishi, S. Saito, and S. Yamamoto, Astron. Astrophys. **317**, L1 (1997).
[3]J. Cernicharo, C. Kahane, J. Gómez-González, and M. Guélin, Astron. Astrophys. **164**, L1 (1986).
[4]C. A. Gottlieb, E. W. Gottlieb, and P. Thaddeus, Astron. Astrophys. **164**, L5 (1986).
[5]J. Cernicharo, C. Kahane, J. Gómez-González, and M. Guélin, Astron. Astrophys. **167**, L5 (1986).
[6]J. Cernicharo, M. Guélin, and C. M. Walmsley, Astronom. Astrophys. **172**, L5 (1987).
[7]M. C. McCarthy and P. Thaddeus, J. Chem. Phys. **122**, 174308 (2005).
[8]A. J. Apponi, M. E. Sanz, C. A. Gottlieb, M. C. McCarthy, and P. Thaddeus, Astrophys. J. **547**, 547 (2001).
[9]T. D. Crawford, J. F. Stanton, J. C. Saeh, and H. F. Schaefer III, J. Am. Chem. Soc. **121**, 1902 (1999).
[10]J. Haubrich, M. Mühlhäuser, and S. D. Peyerimhoff, J. Phys. Chem. A **106**, 8201 (2002).
[11]H. Ding, T. Pino, F. Güthe, and J. P. Maier, J. Chem. Phys. **117**, 8362 (2002).
[12]M. Tulej, T. Pino, M. Pachkov, and J. P. Maier, Mol. Phys. **108**, 865 (2010).
[13]J. Haubrich, M. Mühlhäuser, and S. D. Peyerimhoff, J. Mol. Struct. **623**, 335 (2003).
[14]Y. Zhao and D. G. Truhlar, Theor. Chem. Acc. **120**, 215 (2008).
[15]T. H. Dunning, J. Chem. Phys. **90**, 1007 (2003).
[16]M. J. Frisch, G. W. Trucks, H. B. Schlegel, G. E. Scuseria, M. A. Robb, J. R. Cheeseman, G. Scalmani, V. Barone, B. Mennucci, G. Petersson *et al.*, GAUSSIAN 09, Revision D.01, Gaussian Inc., Wallingford, CT, 2009.
[17]J. Finley, P.-A. Malmqvist, B. O. Roos, and L. Serrano-Andres, Chem. Phys. Lett. **288**, 299 (1998).
[18]F. Aquilante, L. De Vico, N. Ferre, G. Ghigo, P.-A. Malmqvist, P. Neogrady, T. B. Pedersen, M. Pitonak, M. Reiher, B. O. Roos, L. Serrano-Andres, M. Urban, V. Veryazov, and R. Lindh, J. Comput. Chem. **31**, 224 (2010).
[19]D. L. Kokkin, N. J. Reilly, R. C. Fortenberry, T. D. Crawford, and M. C. McCarthy, J. Chem. Phys. **141**, 044310 (2014).
[20]C. M. Western, Pgopher, version 7.1.108, University of Bristol, 2010, http://pgopher.chm.bris.ac.uk.
[21]M. E. Jacox, *Vibrational and Electronic Energy Levels of Polyatomic Transient Molecules*, Monograph 3, J. Phys. Chem. Ref. Data (1994).